

## Direct Correlation between Nonrandom Ion Hopping and Network Structure in Ion-Conducting Borophosphate Glasses

D. Zielniok,<sup>1</sup> H. Eckert,<sup>2</sup> and C. Cramer<sup>2,\*</sup>

<sup>1</sup>Fachbereich Chemie der Philipps-Universität Marburg, Hans-Meerwein-Straße, 35043 Marburg, Germany

<sup>2</sup>Institut für Physikalische Chemie and Sonderforschungsbereich 458, Westfälische Wilhelms-Universität, Corrensstraße 28/30, 48149 Münster, Germany

(Received 25 April 2007; revised manuscript received 6 July 2007; published 22 January 2008)

We present temperature-dependent conductivity spectra of sodium borophosphate glasses with a varying borate/phosphate ratio but a constant sodium oxide content which can be mapped into time-dependent mean square displacements. For the first time, we show that characteristic lengths of ion transport derived thereof are directly linked to features of network structure, viz., the number of boron oxide tetrahedra. Our results also shed light on the mixed network former effect.

DOI: 10.1103/PhysRevLett.100.035901

PACS numbers: 66.30.hh, 61.43.Fs, 66.30.Dn

ac conductivity spectra probe ion movements on different time and length scales [1]. At low frequencies, conductivity spectra typically show a “dc regime,” where the conductivity,  $\sigma_{dc}$ , is independent of frequency.  $\sigma_{dc}$  reflects the long-range ion transport resulting from consecutive jumps where ions leave their sites successfully. At higher frequencies where the conductivity,  $\sigma(\nu)$ , increases with frequency  $\nu$ , ionic movements are probed on smaller length scales. Here, the ionic dynamics is characterized by nonrandom, correlated forward-backward movements [2]. Several models have been developed to explain the shape of  $\sigma(\nu)$ , see, e.g., Refs. [3]. These models give different insights into general hopping mechanisms, but structural details are not considered.

Several approaches have been proposed to learn something about the length scales of ion transport. Martin [4], e.g., calculated jump distances for ion-conducting glasses from density values assuming a homogeneous distribution of cation sites and connected them with the activation energy of the dc conductivity. As far as a direct derivation of length scales from  $\sigma(\nu)$  is concerned (an approach also used in this Letter), Sidebottom *et al.* [5] were the first in 1997 who analyzed conductivity spectra with respect to characteristic length scales of the ion transport and their relation to structural features of the glasses. They determined a “typical length scale representing an average diffusional displacement of an ion per activated jump” which can be correlated to properties of the glass host. For various glasses, they found a linear relation between this quantity and the average distance between the mobile ions which was assumed to be proportional to  $y^{-1/3}$ , where  $y$  is the alkali oxide content in mol% [5]. Later, Sidebottom showed that length scales characterizing ion transport in disordered materials depend upon the dimensionality of the conducting space [6].

In 1999, Roling *et al.* [7] were the first who obtained absolute values for the time-dependent mean square displacements (MSD) of the mobile ions from a combined analysis of experimental dynamic conductivities and tracer

diffusion data using linear response theory. They investigated sodium germanate glasses with varying ion content and showed that the linear relation between characteristic length scales derived from the MSD and interionic separation distances is only valid at low sodium contents. For high sodium contents, these lengths decrease with sodium content stronger than linearly. They concluded that the latter result might be due to structural changes in the glass matrix. This conclusion was later supported by other results [8], where the authors compared characteristic lengths derived from the MSD of germanate, borate and silicate glasses with strongly varying ion content. They concluded that the depolymerization of the network due to the formation of nonbridging oxygens is very likely to cause the strong decrease of the spatial extent of the nonrandom ion hopping at high cation contents.

In 2004, Funke and Banhatti showed that characteristic length scales of ion hopping can also be deduced from the MIGRATION concept [9,10]. In Ref. [10], they reanalyzed conductivity and permittivity data of Ref. [7]. With a slightly different definition of a characteristic localized mean displacement and assuming that the Haven ratio is one, they found a validity of the linear relation between the characteristic localized mean square displacement and  $y^{-1/3}$  also at sodium oxide contents where Roling *et al.* had reported deviations [7].

The work up to date, which focuses on glass systems with strongly varying ion content, shows that the length scales characterizing the ion transport somehow depend on the glass structure. However, changes of the ion content go hand in hand with changes of the glass network as the number of negative network countercharges increases with cation content. Changes due to a varying ion number density and to accompanying structural changes can therefore not be separated.

Here, we report on a new approach on studying the mixed network former effect by determining local length scales of ionic motion from conductivity spectra. A comparison with structural information obtained by NMR

spectroscopy is made. Mixed network former effects have also been found in other glass systems, see, e.g., Refs. [11,12]. Similar to our work, the mixed network former effect has been earlier studied simultaneously by NMR and dynamic conductivity measurements, yielding information on both the structure and the dynamics, see Ref. [11]. For the studied lithium silicophosphate glasses, the authors could show that the activation enthalpy of the dc conductivity characterizing the macroscopic transport shows a mixed network former effect; however, no length scales of ionic motions connectable to structural features of the glasses were derived from  $\sigma(\nu)$ .

We now show for the first time that there is a direct correlation between characteristic length scales of ion movements and the number of  $\text{BO}_4$  tetrahedra in different borophosphate glasses with almost constant cation number densities. The structure of the glass system  $0.4\text{Na}_2\text{O} \cdot 0.6[x\text{B}_2\text{O}_3 \cdot (1-x)\text{P}_2\text{O}_5]$  (with  $0.0 \leq x \leq 1.0$ ) was simultaneously studied by NMR and Raman spectroscopy [13]. To study the ion dynamics in these glasses, we recorded wide-range ac conductivities at frequencies between  $10^{-2}$  and  $10^6$  Hz and at various temperatures between 173 and 548 K, see also Ref. [13]. As we calculated the time-dependent mean square displacement (MSD) directly from experimental conductivities following the procedure published by Roling *et al.* [7,8] (which only involves linear response theory), *our results do not depend on any model assumptions*. We show for glassy  $0.4\text{Na}_2\text{O} \cdot 0.6[x\text{B}_2\text{O}_3 \cdot (1-x)\text{P}_2\text{O}_5]$  that (i) The different conductivity isotherms of a given glass ( $x = \text{const}$ ) follow the time-temperature superposition principle and can be scaled onto a master curve. This implies that the overall underlying ionic hopping mechanism does not change with temperature. This result for mixed network former glasses contrasts the finding for mixed cation glasses where the shape of the conductivity spectra depends on temperature [14]. (ii) From the conductivity master curves of the various glass compositions, we can calculate time-dependent mean square displacements of the center of ion charge according to Ref. [7,8]. Furthermore, characteristic length scales of ionic motions are derived at respective characteristic times; their definition slightly differs from that in Refs. [7,8]. (iii) These characteristic length scales of ion movements show a mixed network former effect. (iv) The variations of the characteristic length scales with composition are strongly correlated with the number of boron oxide tetrahedra determined from NMR spectroscopy [13].

Figure 1(a) is a log-log plot of the real part of the complex conductivity versus frequency of glassy  $0.4\text{Na}_2\text{O} \cdot 0.6[x\text{B}_2\text{O}_3 \cdot (1-x)\text{P}_2\text{O}_5]$  with  $x = 0.0$ . Similar spectra were obtained for all other compositions ranging from  $x = 0.1$  to 1.0. All spectra show frequency and temperature dependences which are typical of most ion conductors. At low frequencies and at sufficiently high temperatures, we see a dc regime, where  $\sigma_{\text{dc}}T$  is Arrhenius activated. With increasing temperature, the onset of dispersion defined by  $\sigma(\nu^*)/\sigma_{\text{dc}} = 2$  shifts to higher frequen-

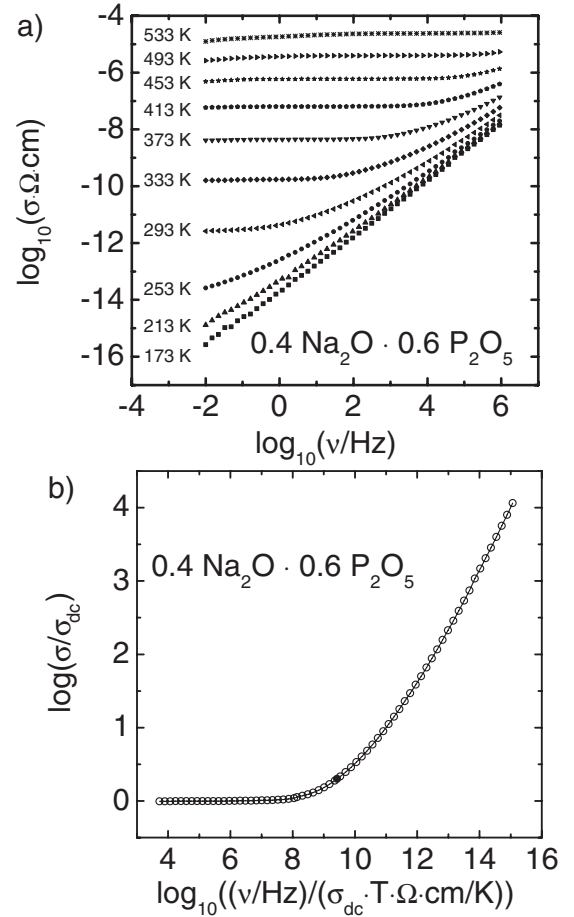


FIG. 1. (a) Experimental conductivities of glassy  $0.4\text{Na}_2\text{O} \cdot 0.6\text{P}_2\text{O}_5$  at various temperatures and (b) master curve derived thereof. The error is within the symbol size.

cies. Like in many other glasses, the so defined onset frequency  $\nu^*$  has the same activation enthalpy as  $\sigma_{\text{dc}}T$ . Figure 1(b) shows a master curve constructed from different conductivity isotherms employing the Summerfield scaling formalism [15]. The full circle in Fig. 1(b) marks the onset of dispersion at the normalized onset frequency  $\nu^*_{\text{norm}} = \nu^*/(\sigma_{\text{dc}}T)$  with  $\sigma^*_{\text{norm}} = \sigma(\nu^*)/\sigma_{\text{dc}} = 2$ . Summerfield scaling is also valid for all other glass compositions not presented here. The shape of the master curves is independent of composition, but the position of the dispersion onset on the normalized frequency scale varies.

According to the following equation, conductivity spectra can be transformed into the mean square displacement of the mobile ions  $\langle r^2(t) \rangle$  [7,8]:

$$\begin{aligned} \langle r^2(t) \rangle &= \frac{12k_B T H_R}{N_v q^2 \pi} \int_0^t dt' \int_0^\infty \frac{\sigma(\nu)}{\nu} \sin(2\pi\nu t') d\nu \\ &= \langle R^2(t) \rangle H_R. \end{aligned} \quad (1)$$

$\langle R^2(t) \rangle$  in Eq. (1) is the mean-square displacement of the center of charge of the mobile ions which is connected with the mean square displacement of the mobile ions via the

Haven ratio  $H_R$  [7,8]. As the Haven ratio is not known for our glasses, we have determined the displacement of the center of charge of the mobile ions as defined in Eq. (1). In ion-conducting glasses,  $H_R$  is normally between 0.2 and 0.3 for moderately large alkali contents (>30 mol%) and nearly unity for very small ion contents (<1 mol%) [5,16]. As the ion content is constant (40 mol%) in all of our glasses, we can assume that  $H_R$  will not significantly change with composition. In a good approximation, the MSD of the mobile ions  $\langle r^2(t) \rangle$  will therefore show the same dependence on composition as  $\langle R^2(t) \rangle$ .

Figure 2 displays  $\langle R^2(t) \rangle$  values calculated from the conductivity master curve presented in Fig. 1(b), analogously to Roling *et al.*'s procedure [7,8]. At long times,  $\langle R^2(t) \rangle$  reflects the diffusive behavior of the mobile ions, where  $\langle R^2(t) \rangle$  is proportional to time. At shorter times, we see the so-called subdiffusive regime where the increase of  $\langle R^2(t) \rangle$  with time is weaker than linear. This regime is due to nonrandom forward-backward ion movements on a shorter time scale  $t$  which is connected to the experimental frequency by  $t = 1/(2\pi\nu)$ . Therefore, the normalized frequency scale of Fig. 2 is given by:  $t_{\text{norm}} = 1/(2\pi\nu_{\text{norm}}) = \sigma_{\text{dc}}T/(2\pi\nu) = \sigma_{\text{dc}}Tt$ . Figure 2 implies that  $\langle R^2(t) \rangle$  as a function of  $t\sigma_{\text{dc}}T$  is independent of temperature. This means that the position of  $\langle R^2(t) \rangle$  on the time scale depends on temperature, while the value of  $\langle R^2(t) \rangle$  at characteristic points of the curves is independent of temperature. In the following, we will use the point marked by the filled circle in Fig. 2 [which corresponds to the marked onset point in Fig. 1(b)] as a measure for a length scale characterizing the transition between the diffusive and subdiffusive ion dynamics. In analogy to Ref. [8], we define a characteristic length, viz.  $\sqrt{\langle R^2(t^*) \rangle}$ , in which  $t^*$  is given by  $t^* = 1/(2\pi\nu^*)$ . This quantity is then determined for all compositions of glassy  $0.4\text{Na}_2\text{O} \cdot 0.6[x\text{B}_2\text{O}_3 \cdot (1-x)\text{P}_2\text{O}_5]$ . The resulting  $\sqrt{\langle R^2(t^*) \rangle}$  values are displayed in Fig. 3(a) as a function of the borate content  $x$ . The data clearly show a mixed network former effect

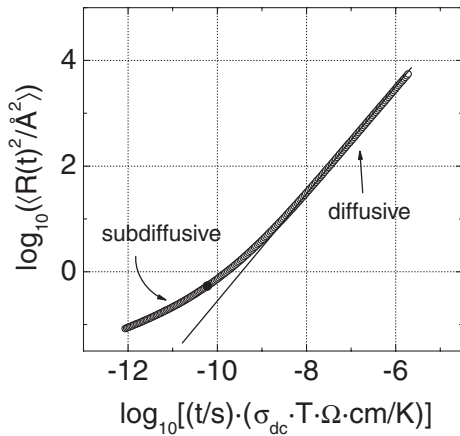


FIG. 2. Mean square displacements  $\langle R^2(t) \rangle$  (error within 2%) derived from the master curve presented in Fig. 1(b).

with two maxima and an intermediate local minimum occurring at  $x = 0.6$ . In contrast to the glass systems studied in Refs. [7,8], the composition dependence of  $\sqrt{\langle R^2(t^*) \rangle}$  cannot be traced back to a variation of the sodium ion content, as this is approximately constant in all of our samples, but must instead be related to structural changes occurring as  $\text{P}_2\text{O}_5$  is replaced by  $\text{B}_2\text{O}_3$ . These structural changes are not directly reflected in the macroscopic density nor in the molar volume calculated thereof. The density values of our glasses published in Ref. [13] show a linear increase as  $x$  is changed from 0 to 0.4, and then at higher  $x$ -values, a linear decrease. The molar volume decreases continuously with  $x$  in an almost linear fashion. So neither the macroscopic density nor the molar volume shows the special kind of mixed network former effect seen in  $\sqrt{\langle R^2(t^*) \rangle}$ . This clearly indicates that the composition dependence of  $\sqrt{\langle R^2(t^*) \rangle}$  is not simply due to a change in free volume accompanied by dilution of characteristic sites, but must be connected to a more complicated change in the microscopic glass structure. A detailed study on the glass structure of borophosphate glasses

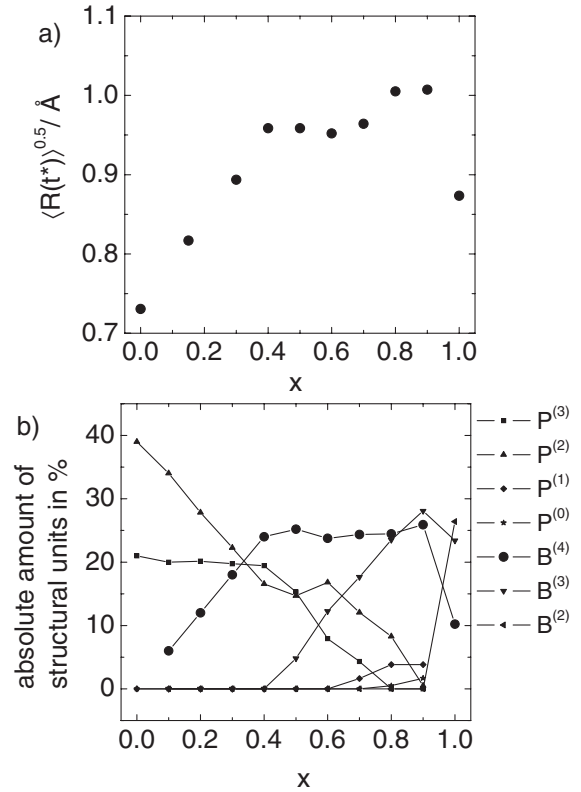


FIG. 3. (a) Lengths depending on the spatial extent of non-random diffusion ( $\sqrt{\langle R^2(t^*) \rangle}$ ) (error within 1%) of glassy  $0.4\text{Na}_2\text{O} \cdot 0.6[x\text{B}_2\text{O}_3 \cdot (1-x)\text{P}_2\text{O}_5]$ . (b) Structural units and their abundance in borophosphate glasses [13]. The numbers in brackets in the structural units specify the number of bridging oxygen atoms.  $\text{BO}_4$  units are highlighted by larger symbols. Error bars are omitted for the sake of clarity; estimated precision of the site species concentrations are  $\pm 2\%$ .

is presented in Ref. [13]. Using  $^{11}\text{B}$ - and  $^{31}\text{P}$ -MAS-NMR, we obtained the population of various structural phosphate and borate units present in the glasses, see also Fig. 3(b). This figure shows that the number of tetrahedrally coordinated borate groups shows the same composition dependence as  $\sqrt{\langle R^2(t^*) \rangle}$ .

As outlined before, Roling *et al.* reported that the spatial extent of the nonrandom local ion movements depends on the degree of depolymerization of the glass network by forming of nonbridging oxygens [7,8]. This conclusion was reached because in strongly depolymerized glasses, the length scale characterizing the spatial extent of local nonrandom ion movements decreases faster with increasing alkali content than in glasses with highly polymerized networks. However, no quantitative relation between the characteristic length scale and any structural feature was given in Refs. [7,8]. In addition, influences of varying ion content and structural changes on the characteristic lengths could not be separated. Our results now show a direct relation between  $\sqrt{\langle R^2(t^*) \rangle}$  and the number of  $\text{BO}_4$  tetrahedra which we have quantified by NMR techniques [13]. Because of the constant  $\text{Na}^+$  content, we could study purely structural aspects influencing  $\sqrt{\langle R^2(t^*) \rangle}$ . Our results show that high concentrations of  $\text{BO}_4$ -tetrahedra, which increase the network connectivity, lead to an increase in the characteristic distance  $\sqrt{\langle R^2(t^*) \rangle}$ , strongly confirming the conclusions of Roling *et al.* [7,8]. Whereas  $\sqrt{\langle R^2(t^*) \rangle}$  is connected with length scales where the ions move nonrandomly exploring their *local environment*,  $\sigma_{\text{dc}}$  is determined by consecutive successful ion hops resulting in *macroscopic ion transport*. The fact that the values of the dc conductivities at constant temperature feature the same composition dependence [13] as  $\sqrt{\langle R^2(t^*) \rangle}$  implies that the macroscopic ion transport properties are strongly interrelated to the ion dynamics on smaller length scales. Thus, in our case,  $\text{BO}_4$  tetrahedra facilitate the  $\text{Na}^+$  transport on microscopic and macroscopic length scales. For the binary sodium borate glass ( $x = 1$ ),  $\sqrt{\langle R^2(t^*) \rangle}$  is significantly smaller than in other glasses with high boron content, see Fig. 3(a). This can be explained by the formation of borate groups with nonbridging oxygen which act as “Coulomb traps” for the  $\text{Na}^+$  ions causing a decrease of  $\sqrt{\langle R^2(t^*) \rangle}$ . We think that anionic  $\text{BO}_4$  groups are favorable for ion transport because their negative charge is dispersed over four boron-oxygen bonds, thereby diminishing Coulomb forces.

In this Letter, we could show that in sodium borophosphate glasses, the nonrandom forward-backward ion dynamics on short length scales is not only strongly correlated to the macroscopic transport on longer length scales, but also to changes in the glass structure, viz., the number of  $\text{BO}_4$  tetrahedra. Thus, the formation of  $\text{BO}_4$  units plays a significant role in the conduction process of the  $\text{Na}^+$  ions. We also conclude that in our borophosphate glasses, the origin of the mixed network former effect is

directly linked to the increased formation of  $\text{BO}_4$  tetrahedra caused by the interactions of the two network formers.

We thank R. D. Banhatti, K. Funke, and B. Roling for many stimulating discussions.

\*Corresponding Author

- [1] K. Funke and C. Cramer, *Curr. Opin. Solid State Mater. Sci.* **2**, 483 (1997).
- [2] K. Funke, *Prog. Solid State Chem.* **22**, 111 (1993); P. Maass, J. Petersen, A. Bunde, W. Dieterich, and H.E. Roman, *Phys. Rev. Lett.* **66**, 52 (1991).
- [3] K.L. Ngai *Comments Solid State Phys.* **9**, 127 (1979); K.L. Ngai *Comments Solid State Phys.* **9**, 141 (1980); S.R. Elliott and A.P. Owens, *Ber. Bunsen-Ges. Phys. Chem.* **95**, 987 (1991); D. Knödler, P. Penzig, and W. Dieterich, *Solid State Ionics* **86–88**, 29 (1996); P. Maass, B. Rinn, and W. Schirmacher, *Philos. Mag. B* **79**, 1915 (1999); T.B. Schrølder and J.C. Dyre, *Phys. Rev. Lett.* **84**, 310 (2000); B. Roling, *Phys. Chem. Chem. Phys.* **3**, 5093 (2001); K. Funke and R. D. Banhatti, *Mater. Res. Soc. Symp. Proc.* **756**, 3 (2003) and references given in these papers.
- [4] S. W. Martin, *J. Am. Ceram. Soc.* **71**, 438 (1988).
- [5] D.L. Sidebottom, P.F. Green, and R.K. Brow, *J. Non-Cryst. Solids* **222**, 354 (1997).
- [6] D.L. Sidebottom, *Phys. Rev. Lett.* **83**, 983 (1999).
- [7] B. Roling, C. Martiny, and K. Funke, *J. Non-Cryst. Solids* **249**, 201 (1999).
- [8] B. Roling, C. Martiny, and S. Brückner, *Phys. Rev. B* **63**, 214203 (2001).
- [9] K. Funke and R. D. Banhatti, *Solid State Ionics* **169**, 1 (2004).
- [10] R. D. Banhatti and K. Funke, *Solid State Ionics* **175**, 661 (2004).
- [11] O. Kanert, R. Kuchler, J. Peters, A. Volmari, H. Jain. H. Eckert, and E. Ratai, *J. Non-Cryst. Solids* **222**, 321 (1997); V. Blache, J. Förster, H. Jain, O. Kanert, R. Kuchler, and K.L. Ngai, *Solid State Ionics* **113–115**, 723 (1998) an references given in these papers.
- [12] F. Branda, A. Costantini, R. Fresa, and A. Buri, *Phys. Chem. Glasses* **36**, 272 (1995); A. Costantini, A. Buri, and F. Branda, *Solid State Ionics* **67**, 175 (1994); J.F. Duce and J.J. Videau, *Mater. Lett.* **13**, 271 (1992); J.J. Videau, J.F. Duce, K. S. Suh, and J. Senegas, *J. Alloys Compd.* **188**, 157 (1992); S. Kumar, P. Vinatier, A. Levasseur, and K.J. Rao, *J. Solid State Chem.* **177**, 1723 (2004); H. Eckert, *Prog. NMR Spectroscopy* **24**, 159 (1992) and references given therein.
- [13] D. Zielniok, C. Cramer, and H. Eckert, *Chem. Mater.* **19**, 3162 (2007).
- [14] C. Cramer, S. Brückner, Y. Gao, and K. Funke, *Phys. Chem. Chem. Phys.* **4**, 3214 (2002).
- [15] S. Summerfield, P.N. Butcher, *J. Non-Cryst. Solids* **77–78**, 135 (1985); S. Summerfield, *Philos. Mag. B* **52**, 9 (1985).
- [16] H. Jain, N.L. Peterson, and H.L. Downing *J. Non-Cryst. Solids* **55**, 283 (1983); J.N. Mundy and G.L. Jin, *Solid State Ionics* **21**, 305 (1986); H. Kahnt, *Ber. Bunsen-Ges. Phys. Chem.* **95**, 1021 (1991).